The fracture behavior of SiC/Cu interpenetrating phase nanocomposites: A molecular dynamics study

S. Shadlou* and L.D. Wegner**

* University of Saskatchewan, 57 Campus Drive
Saskatoon, SK S7N 5A9, Canada, shahin.shadlou@usask.ca
** University of Saskatchewan, 57 Campus Drive
Saskatoon, SK S7N 5A9, Canada, leon.wegner@usask.ca

ABSTRACT

In the present study, the effect of various parameters on the fracture behavior of SiC at atomic scale is studied by using molecular dynamics (MD) method. The parameters such as crack orientation, temperature, presence of a Cu (as a ductile phase), and the volume fraction of the Cu are studied. The presence of Cu phases is found to be very effective method for increasing the ductility of ceramics even at low volume fractions of Cu. However, the efficacy of Cu phase fades out as the temperature increases. Three low-index crack surfaces including (110), (111), and (100) in crystalline 3C-SiC are investigated and it is found that the fracture energy and crack growth direction is totally dependent on the crack orientation and the crack propagation could be totally different for different planes of crack.

Keywords: Molecular Dynamics, Crack Growth, Fracture, SiC, Cu, Nano-composite

1 INTRODUCTION

Owing to their high strength, good abrasion resistance, low density, high melting temperature, and other interesting characteristics, ceramics have been extensively used in a wide range of industries [1]. However, one of the major drawbacks of the ceramics is low fracture toughness. To address this issue, several studies have been conducted. One of the very effective means is using ceramics along with a second ductile phase to address this issue. This is a new class of composites with three dimensional, interconnected microstructural networks of the constituents was introduced which are referred to as interpenetrating phase composites (IPCs) or co-continuous composites. With advancement in manufacturing at the nano scale, it is now vital to have an in-depth understanding of the effective mechanisms and behavior of IPCs at that scale [2,3].

2 MOLECULAR DYNAMICS SIMULATION

A cubic cell model was used to simulate the nano-structure of a SiC/Cu IPC nanocomposite. Generally, two different models were investigate namely: (i) pure SiC and (ii) SiC/Cu. In all models the dimensions of the cubic cell model is 300×300×25 A and each model contains about 200,000 atoms. All models contain a pre-crack with length of 30A at three different orientations of (001), (110) and (111). A schematic of the SiC and SiC/Cu models are depicted in Figure 1.

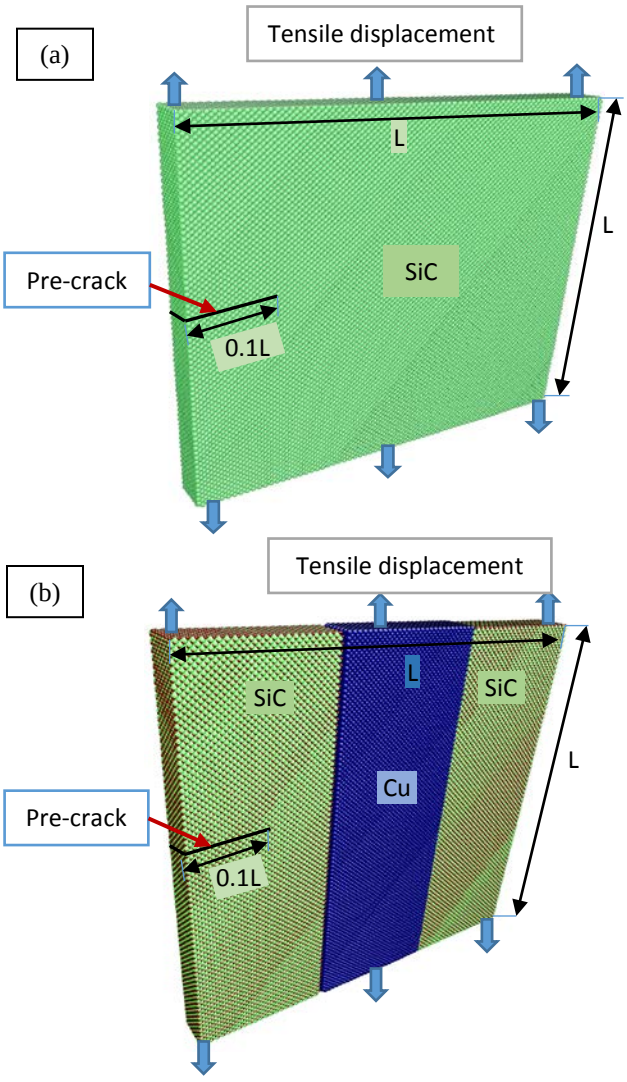

Figure 1: schematic of (a) SiC and (b) SiC/Cu (1/3 vol%) models with fracture plane of (001)

The MD simulation was conducted using LAMMPS [4], an open source code which provides computational infrastructure for massive parallel particle simulations. All visuals of the molecular and crystal structure were created using AtomEye [5]. Different force fields were used to describe the interaction between different atoms. The Tersoff potential [6] was used to simulate the interaction between Si and C atoms. The embedded-atom method (EAM) potential [7] was also used to govern the interaction of Cu atoms. The parameters suggested by Zhang et al. [8] for Tersoff potential were employed to describe the interactions between Cu and Si atoms. Finally, Morse potential was adopted to define the interaction between Cu and C atoms [9].

The NPT ensemble was employed for all the simulations. The Verlet numerical method [10] was utilized to integrate Newton's equations of motion. A time step of 1 fs was used for integration of equations. Before conducting each simulation, the model was first relaxed for 50 ps at the target temperature. Then the models were subjected to a uniform strain in one of the axis directions over several steps. The mean stress of the atomic system was calculated at the last 0.2 ps of each step. The average stresses in the atomistic systems were calculated using the virial theorem [11,12].

3 RESULTS AND DISCUSSION

The crack growth paths in pure SiC (PS) and in SiC/Cu nanocomposite (SCN) are compared in Figure 2. As can be seen, for PS after critical strain the crack starts growing and moves forward throughout the crystal. However, for SCN the crack grows until it reach to the ductile Cu phase and gets arrested. Then it starts growing in the Cu phase with much lower speeds. However, before it travels through the Cu phase the other part of SiC (on the right-hand side) undergoes fast fracture. Given the large difference between the stiffness and ultimate strength of Cu and SiC, total separation in the SiC phase can be considered as final fracture of SCN. This fashion of fracture can be seen in the stress—strain behavior of these materials as shown in Figure 3(a). For PS the stress drops to zero short after crack initiation. On the other hand, for SCN after the crack initiation the stress drops to about 50% of maximum and then it increases up to the fast fracture of the second part of SiC.

The crack growth velocity (CGW) in the SiC phase for all models are depicted in Figure 3(b). The reported CGW is calculated based on the average velocity inside the SiC phase only from the moment of crack growth initiation up to the full fracture. In case of SCN, to calculate CGW, only the average velocity in the left-hand side SiC is considered. The velocities for PS agrees with the data reported in [13]. It is noteworthy that the accuracy of the data for crack growth velocity depends on the intervals between the recorded data of the model status. In the present study this interval is strain of 0.00038. Given the very fast crack growth velocity, it is possible that with a shorter interval of recording data, the results would be slightly different.

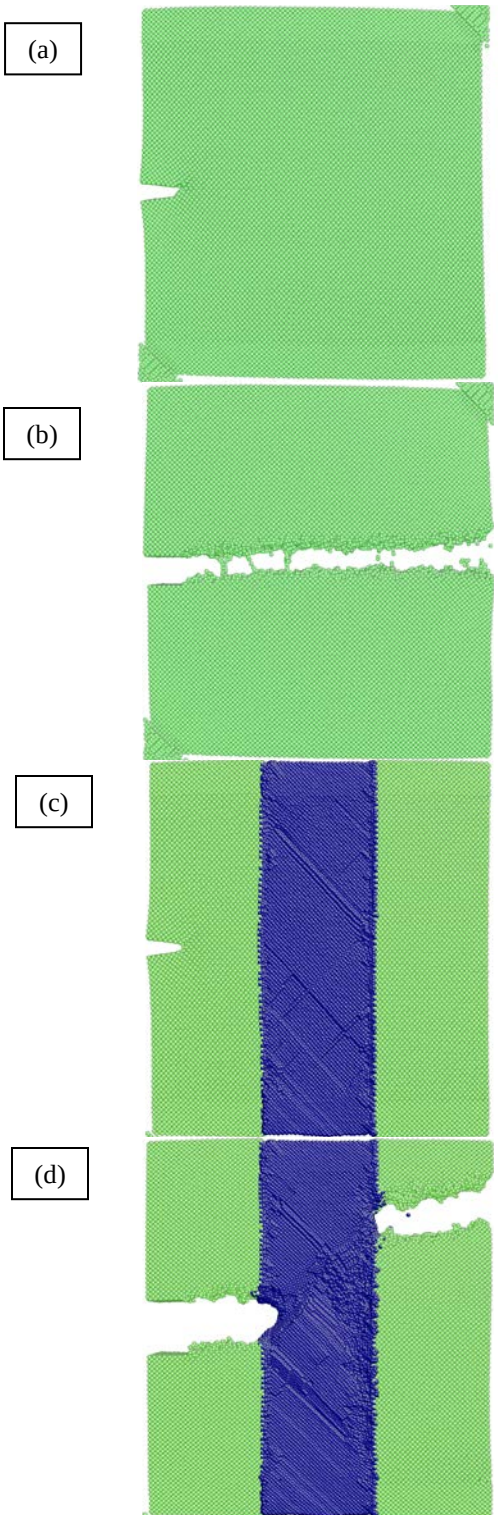

Figure 2: crack growth path on (001) plane for pure SiC at the strain of (a) 0.095, (b) 0.101 and SiC/Cu nanocomposite at the strains of (c) 0.911, (d) 0.197

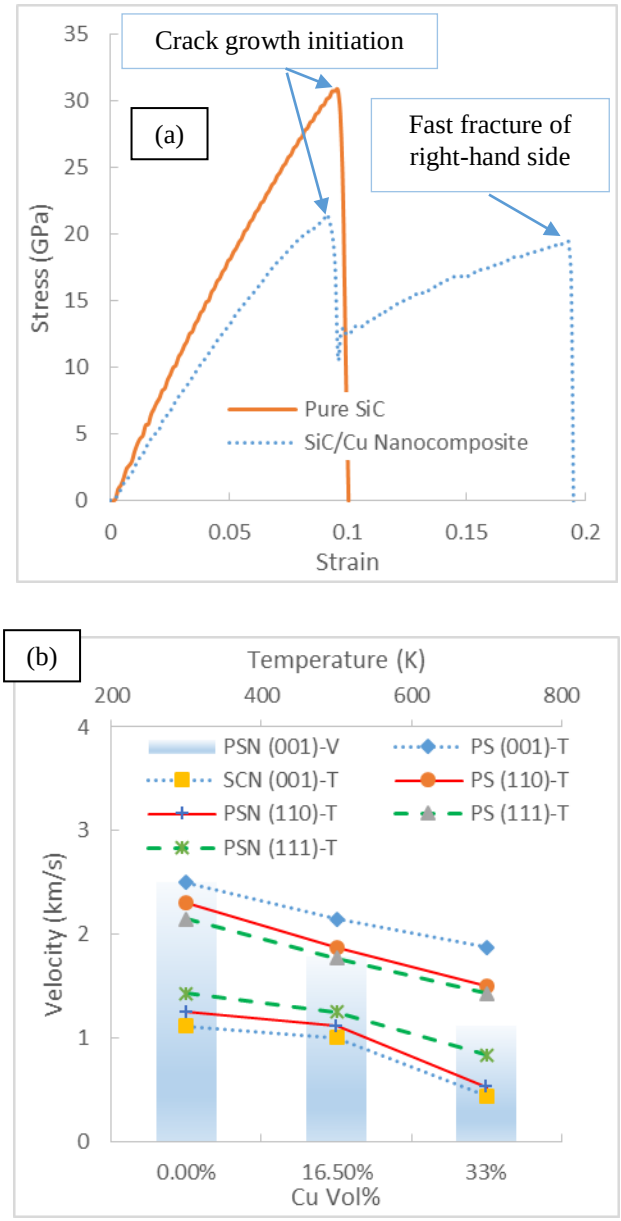

Figure 3: (a) Typical stress—strain curve for PS and SCN for crack on (001) plane (b) crack growth velocity in SiC phase at different temperatures (In the legend, the ending of "T" indicates the effect of temperature and ending of "V" is an indicator of effect of volume fraction).

As expected, by increasing the temperature CGV decreases. For PSs there is a linear trend of decreasing CGV with increasing the temperature. However, for SCNs while there is not a large difference between 300 K and 500 K, the CGV drops at higher rates when increasing the temperature from 500 K to 700 K. This trend can be attributed to the fact that presence of SiC phase and increasing the temperature increases the ductility of the model. Therefore, concurrent presence of both these factors could lead to decrease of their efficacy especially at lower amount of temperature increase. Comparing the results indicates that presence of the Cu phase has a much more effective impact on the CGW compared with increasing the temperature. While the increase in the temperature could lead to about 20% decrease in CGW presence of the ductile phase (i.e., Cu) can decrease the CGW up to 50%, which indicates that the later method is much more efficient.

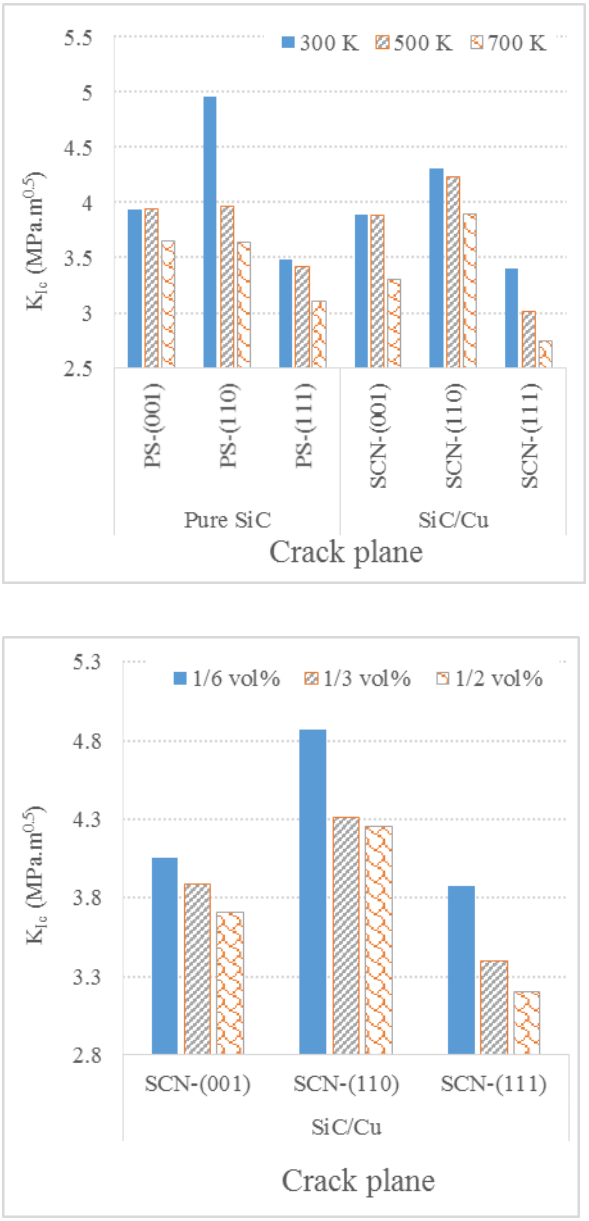

Figure 4: The change in the fracture toughness values of the models with (a) Temperature, (b) Volume fraction of the SiC phase.

The fracture toughness of different models were calculated and depicted in Figure 4. The average of fracture toughness

for PS is about 4 MPa.m0.5 which is in good agreement with previously reported values [14]. As can be seen, depending on the plane of initial crack, the fracture toughness values in PS could be different. The highest fracture toughness was observed in the PS-(110) model and lowest fracture toughness was calculated for the PS-(111) model. This can be attributed to the relatively lower surface energy of the (111) plane [13,14]. Different fracture planes could either lead to cleavage fracture or dislocation emission. The latter causes a plastic deformation at the crack tip and dissipate more energy which leads to higher fracture toughness.

Comparing the fracture toughness of the PS models for different planes with those of the SCN models shows that in general presence of the softer phase decreases the fracture toughness. However, it can be seen that except for PS-(110) for other planes there is not a large difference between the PS models and the SCN models. Moreover, higher temperatures and larger volume fractions of Cu also resulted in lower fracture toughness. This decrease in the fracture toughness of the models is a result of drop in the equivalent stiffness of the model which is either because of presence of a second phase with lower stiffness or increasing the temperature. It can be concluded that while higher temperatures and larger volume fractions of Cu would increase the ductility of the model, at the same time they decrease the fracture toughness. Thus, in the design of such materials the must be balance between desired ductility and fracture toughness.

4 CONCLUSIONS

The results showed that the fracture behavior of SiC can be totally different depending on the plane of initial crack. The (111) plane has the lowest surface energy which makes the crack growth in this plane much easier. It was also found that the presence of a second ductile phase (i.e., Cu) can highly affect the fracture behavior of SiC. Not only the Cu phase slows down the crack growth speed in the SiC medium, it also arrests the crack growth which highly increases the toughness of the material.

Calculating the fracture toughness of materials indicated that the by adding a ductile phase to SiC the fracture toughness decreases. This can be attributed to the fact that the equivalent stiffness of the model drops. Increasing the temperature and volume fraction of the Cu phase increases the ductility of the model and at the expense of reducing the equivalent stiffness of the model. Therefore, in designing IPC nanocomposites, it is important to have an in-depth understanding of the effect of different factors to best tailor the desired properties.

REFERENCES

[1] A. Okada, J. Eur. Ceram. Soc. 28 (2008) 1097–1104.
[2] P.S. Branicio, J. Comput. Theor. Nanosci. 9 (2012) 1870–1880.
[3] S. Shadlou, L.D. Wegner, Comput. Mater. Sci. 117 (2016) 428–436.
[4] S. Plimpton, Jounal Comput. Phys. 117 (1995) 1–42.
[5] J. Li, Model. Simul. Mater. Sci. Eng. 11 (2003) 173–177.
[6] J. Tersoff, Phys. Rev. B 39 (1989) 5566–5568.
[7] Y. Mishin, M. Mehl, D. Papaconstantopoulos, a. Voter, J. Kress, Phys. Rev. B 63 (2001) 1–16.
[8] J. Zhang, C. Liu, Y. Shu, J. Fan, Appl. Surf. Sci. 261 (2012) 690–696.
[9] K. Maekawa, A. Itoh, Wear 188 (1995) 115–122.
[10] L. Verlet, Phys. Rev. 159 (1967) 98–103.
[11] M. Zhou, Proc. R. Soc. A Math. Phys. Eng. Sci. 459 (2003) 2347–2392.
[12] K.S. Cheung, S. Yip, J. Appl. Phys. 70 (1991) 5688–5690.
[13] D. Sen, C. Thaulow, S. V. Schieffer, A. Cohen, M.J. Buehler, Phys. Rev. Lett. 104 (2010) 235502.
[14] K.W.K. Leung, Z.L. Pan, D.H. Warner, Acta Mater. 77 (2014) 324–334.